



Deep Space Network

103 34-m HEF Subnet Telecommunications Interface

Document Owner:

Approved by:

Signature Provided 07/10/2014

Signature Provided 07/10/2014

Stephen D. Slobin Date
Antenna System Engineer

Timothy Pham Date
Communications Systems Chief
Engineer

Prepared by:

Released by:

Signature Provided 07/10/2014

Signature Provided 08/01/2014

Stephen D. Slobin Date
Antenna System Engineer

Christine Chang Date
DSN Document Release Authority

DSN No. **810-005, 103, Rev. C**
Issue Date: August 01, 2014
JPL D-19379

Jet Propulsion Laboratory
California Institute of Technology

*Users must ensure that they are using the current version in DSN Telecommunications Link Design Handbook website:
<http://deepspace.jpl.nasa.gov/dsndocs/810-005/>*

© <2014> California Institute of Technology.
U.S. Government sponsorship acknowledged.

Review Acknowledgment

By signing below, the signatories acknowledge that they have reviewed this document and provided comments, if any, to the signatories on the Cover Page.

Signature Provided

07/10/2014

Signature Not Provided

Jeff Berner
DSN Project Chief Engineer

Date

David Rochblatt
Antenna System Engineer

Date

Document Change Log

Rev	Issue Date	Prepared By	Affected Sections or pages	Change Summary
Initial	11/30/2000	Stephen Slobin Robert Sniffin	All	New Module
A	04/02/2007	Stephen Slobin Robert Sniffin	ALL	Documents installation of a 200 W S-band uplink at DSS-45 and DSS-65. Revised <i>TAMW</i> formulation for noise temperature to be consistent with Rev. B of module 105.
B	09/19/2008	Stephen Slobin Robert Sniffin	2. Table 1 & 2	Provides measured performance of S-band uplink at DSS 45 and DSS 65 and editorial changes.
C	08/01/2014	Stephen Slobin	Table 1 Table 3 Table 4 Table 5 Table A-3 Figure 1a Figure 1b Figure 7	Updated to include DSS-15 S-band transmitter. New DSS-15 Tamw for X-band dual-HEMT feed. New DSS-15/45/65 Tamw for low-gain mode. New wind-effect gain model. New Tamw and Top for DSS-15/45/65 X-band. New T1, T2, a for DSS-15/45/65 X-band. New for DSS-15. Re-numbered to include DSS-45/65 only. New noise temperatures for DSS-15 X-band.

Contents

<u>Paragraph</u>	<u>Page</u>
1 Introduction.....	7
1.1 Purpose.....	7
1.2 Scope.....	7
2 General Information.....	7
2.1 Telecommunications Parameters	8
2.1.1 Antenna Gain Variation.....	8
2.1.1.1 Frequency Effects	8
2.1.1.2 Elevation Angle Effects	8
2.1.1.3 Wind Loading	9
2.1.2 System Noise Temperature Variation	9
2.1.3 Pointing Accuracy	10
Appendix A Equations for Modeling.....	28
A.1 Equations for Gain Versus Elevation Angle.....	28
A.2 Equations for System Noise Temperature Versus Elevation Angle	28
A.3 Equation for Gain Reduction Versus Pointing Error	30

Illustrations

<u>Figure</u>	<u>Page</u>
Figure 1a. Functional Block Diagram of the DSS-15 HEF Antenna.....	21
Figure 1b. Functional Block Diagram of the DSS-45 and DSS-65 HEF Antennas.....	22
Figure 2. S-Band Receive Gain, All HEF Antennas, at Feedhorn Aperture.....	23
Figure 3. X-Band Receive Gain, DSS-15 Antenna, at Feedhorn Aperture.....	23
Figure 4. X-Band Receive Gain, DSS-45 Antenna, at Feedhorn Aperture.....	24
Figure 5. X-Band Receive Gain, DSS-65 Antenna, at Feedhorn Aperture.....	24
Figure 6. S-band System Noise Temperature, all HEF Antennas, LNA-1, Non-Diplexed, at Feedhorn Aperture.....	25
Figure 7. X-Band System Noise Temperature, DSS-15, LNA-1, HEMT, RCP, Diplexed at Feedhorn Aperture	25
Figure 8. X-Band System Noise Temperature, DSS-45, LNA-1, Non-Diplexed, at Feedhorn Aperture	26
Figure 9. X-Band System Noise Temperature, DSS-65, LNA-1, Non-Diplexed, at Feedhorn Aperture	26
Figure 10. S-Band Gain Reduction Versus Angle Off Boresight	27
Figure 11. X-Band Gain Reduction Versus Angle Off Boresight.....	27

Tables

<u>Table</u>	<u>Page</u>
Table 1. S-Band Transmit Characteristics	11
Table 2. X-Band Transmit Characteristic	13
Table 3. S- and X-Band Receive Characteristics.....	15
Table 4. Gain Reduction Due to Wind Loading, 34-m HEF Antennas	18
Table 5. T_{AMW} , T_{sky} , and T_{op} for CD=25% Average Clear Weather at Zenith, Referenced to Feedhorn Aperture.....	19

Table A-1. Vacuum Component of Gain Parameters	30
Table A-2. S- and X-Band Year-Average Zenith Atmosphere Attenuation Above Vacuum (<i>AZEN</i>).....	30
Table A-3. Antenna-Microwave Noise Temperature Parameters, Referenced to Feedhorn Aperture	31

1 Introduction

1.1 Purpose

This module provides the performance parameters for the Deep Space Network (DSN) High-efficiency (HEF) 34-meter antennas that are necessary to perform the nominal design of a telecommunications link. It also summarizes the capabilities of these antennas for mission planning purposes and for comparison with other ground station antennas.

1.2 Scope

The scope of this module is limited to providing those parameters that characterize the RF performance of the 34-meter HEF antennas. The parameters do not include effects of weather, such as reduction of system gain and increase in system noise temperature that are common to all antenna types. These are discussed in module 105, Atmospheric and Environmental Effects. This module also does not discuss mechanical restrictions on antenna performance that are covered in module 302, Antenna Positioning, or the effects of terrain masking that are covered in Module 301, Coverage and Geometry.

2 General Information

The DSN 34-m Antenna HEF Subnet contains three 34-meter diameter high-efficiency antennas. These antennas employ an elevation over azimuth (AZ-EL) axis configuration, a single dual-frequency feedhorn, and a dual-shaped reflector design. Although this subnet is referred to as the High-Efficiency Subnet, the efficiency of the antennas is approximately the same as all other DSN antennas. The subnet was constructed when a subnet of lower-efficiency antennas was in existence and the name has been retained. One antenna (DSS-15) is located at Goldstone, California; one (DSS-45) near Canberra, Australia; and one (DSS-65) near Madrid, Spain. The precise station locations are shown in Module 301, Coverage and Geometry.

Block diagrams of the 34-meter HEF microwave and transmitter equipment are shown in Figures 1a (DSS-15) and 1b (DSS-45 and DSS-65). DSS-15 contains new dual X-band HEMTs (one for RCP and one for LCP), while DSS-45 and DSS-65 contain the older X-band maser and X-band HEMT configuration, with RCP and LCP available for each low-noise amplifier (LNA). Additionally, all three antennas offer a low-gain mode (−20 dB) for use at high received signal power levels for spacecraft near the Earth, although test data was available only for DSS-15 and DSS-65. Noise temperatures for DSS-45 in the low-gain mode are engineering estimates, and are indicated by “≈”. An orthomode junction at DSS-45 and DSS-65 for X-band is employed that permits simultaneous RCP and LCP operation, although one polarization will be in the non-diplexed mode and the other will be in the higher-noise diplexed mode. DSS-15 is considered to be always diplexed at X-band, and no lower noise configuration is available. For X-band listen-only operation at DSS-45 and DSS-65, or when transmitting and receiving on opposite polarizations, the low-noise path (orthomode upper arm) is used for reception. If the

spacecraft receives and transmits simultaneously with the same polarization, the diplexed path must be used and the noise temperature is higher. A waveguide labyrinth is used to couple S-band signals into and out of the feed. This would provide simultaneous RCP and LCP operation although the presence of only one S-band low noise amplifier and receiver channel limits the use to selectable RCP or LCP. At all stations, the S-band polarization selection switch is used to implement a diplexed signal path in addition to the non-diplexed, low-noise signal path.

A 20 kW X-band transmitter is available at all stations. All stations have a 250W S-band transmitter intended for near-Earth spacecraft support as an alternative to the Beam Waveguide (BWG) Subnet 1 described in module 104. In addition to spacecraft tracking, the DSN 34-m Antenna Subnet is also used for very-long baseline interferometry and radio-source catalog maintenance.

2.1 *Telecommunications Parameters*

The significant parameters of the 34-meter HEF antennas that influence telecommunications link design are listed in Tables 1, 2, and 3. Variations in these parameters that are inherent in the design of the antennas are discussed below. Other factors that degrade link performance are discussed in modules 105 (Atmospheric and Environmental Effects) and 106 (Solar Corona and Wind Effects).

2.1.1 *Antenna Gain Variation*

The antenna gains in Tables 1, 2, and 3 do not include the effect of atmospheric attenuation and should be regarded as vacuum gain at the specified reference point.

2.1.1.1 *Frequency Effects*

Antenna gains are specified at the indicated frequency (f_0). For operation at higher frequencies in the same band, the gain (dBi) must be increased by $20 \log (f/f_0)$. For operation at lower frequencies in the same band, the gain must be reduced by $20 \log (f/f_0)$.

2.1.1.2 *Elevation Angle Effects*

Structural deformation causes a reduction in gain whenever the antenna is operated at an elevation angle other than the angle where the reflector panels were aligned. The effective gain of the antenna is also reduced by atmospheric attenuation, which is a function of elevation. Figures 2 through 5 show the estimated gain versus elevation angle for the hypothetical vacuum condition (structural deformation only) and with 0%, 50%, and 90% weather conditions, designated as CD (cumulative distribution) = 0.00, 0.50, and 0.90. A CD of 0.00 (0%) means the minimum weather effect (exceeded 100% of the time). A CD of 0.90 (90%) means that effect which is exceeded only 10% of the time. Qualitatively, a CD of 0.00 corresponds to the driest condition of the atmosphere; a CD of 0.50 corresponds to humid or very light clouds; and 0.90 corresponds to very cloudy, but with no rain. A CD of 0.25 corresponds to average clear weather and often is used when comparing gains of different antennas. Comprehensive S-band and X-band weather effects models (for weather conditions up to 99%

cumulative distribution) are provided in module 105 for detailed design control table use. Equations and parameters for the curves in Figures 2 through 5 are provided in Appendix A.

Figure 2 depicts the S-band (2295 MHz) net gains for all stations as a function of elevation angle and weather condition, including the vacuum condition. Net gain means vacuum-condition gain as reduced by atmosphere attenuation. Figures 3, 4, and 5 present the X-band (8420 MHz) net gains. All gains are referred to the feedhorn aperture, and the equations and parameters of these curves are given in Appendix A. The models use a flat-Earth, horizontally stratified atmosphere approximation.

It should be noted in Appendix A, Table A-1, that the gain parameters do not vary for different configurations (e.g., LNA-1 non-diplexed vs. LNA-1 diplexed), as they do in Table A-3 for the noise temperature parameters. This is due to the fact that the gain is referenced to the feedhorn aperture, and configurations "downstream" (e.g., orthomode and diplexer paths) do not affect the value of gain at the aperture. The observed differences in antenna G/T are attributed only to different values of noise temperature because G and T are both referenced to the feedhorn aperture. When G and T are referenced to the LNA input, both the G and T parameters vary with antenna configuration. When referenced to the feedhorn aperture, only T varies with configuration.

2.1.1.3 Wind Loading

The gain reduction at X-band due to wind loading is listed in Table 4. The tabular data are for structural deformation only and presume that the antenna is maintained on-point by conical scan (CONSCAN, discussed in module 302) or an equivalent process. In addition to structural deformation, wind introduces a pointing error that is related to the antenna elevation angle, the angle between the antenna and the wind, and the wind speed. The effects of pointing error are discussed below. Cumulative probability distributions of wind velocity at Goldstone are given in module 105.

2.1.2 System Noise Temperature Variation

The operating system temperature (T_{op}) varies as a function of elevation angle due to changes in the path length through the atmosphere and ground noise received by the sidelobe pattern of the antenna. Figures 6 through 9 show the combined effects of these factors at S- and X-bands in a hypothetical vacuum (no atmosphere) with no cosmic noise condition for non-diplexed antenna configurations, and with the three weather conditions described above. The equations and parameters for these curves are provided in Appendix A of this module. The models use a flat-Earth, horizontally stratified atmosphere approximation.

This revision of Module 103 presents a new formulation for system operating noise temperature contrasted with the earlier edition. The system operating noise temperature, T_{op} , consists of two parts, an *antenna-microwave component*, T_{AMW} , for the contribution of the antenna and microwave hardware only, and a *sky component*, T_{sky} , that consists of the atmosphere noise plus the cosmic microwave background noise, attenuated by the atmosphere loss. T_{AMW} is shown in Figures 6, 7, 8, and 9 as "ANT-UWV". The previous revision used a term $T_{op,vacuum}$, which included the net cosmic contribution. The atmospheric noise contribution

was added to this to obtain T_{op} . In this revision, the system operating noise temperature is given by

$$T_{op}(\theta) = T_{AMW} + T_{sky} = [T_1 + T_2 e^{-a\theta}] + [T_{atm}(\theta) + T'_{CMB}(\theta)]$$

where

$$T_{sky} = T_{atm}(\theta) + T'_{CMB}(\theta)$$

T_1 , T_2 and a are coefficients and exponent given in Appendix A, Table A-3

T_{atm} is the atmosphere contribution term, calculated from Module 105

T'_{CMB} is the attenuated cosmic contribution, calculated from Module 105

More details of this calculation are given in Appendix A of this module.

Figure 6 shows the S-band (2295 MHz) system noise temperature curves for all three HEF antennas, LNA-1 (HEMT), non-diplexed, referenced to the feedhorn aperture. The S-band atmosphere models are averages of the effects at all three stations, at each CD level. The X-band (8420 MHz) system temperatures referenced to the feedhorn aperture for the three antennas are shown in Figures 7, 8, and 9. Figure 7 shows the noise temperature for DSS-15 with the new LNA-1 RCP HEMT. Figures 8 and 9 show the noise temperatures for DSS-45 and DSS-65 with the antenna in the lowest noise, LNA-1 (maser) non-diplexed configuration. The diplexed configuration higher noise temperatures can be calculated using the parameters given in Appendix A. Separate atmosphere models are used for each station, as given in module 105.

The T_{AMW} noise temperature values in Table 3 are stated with reference to the feedhorn aperture and arise from antenna and microwave hardware contribution only. No atmosphere or cosmic background contribution is included. Table 5 presents values (for all antenna frequencies and configurations, at zenith, with average-clear CD = 0.25 weather) of T_{AMW} , T_{sky} , and T_{op} . The values of T_{sky} in Table 5 are calculated by methods presented in Module 105, Rev. B, using year-average attenuation values in Tables 10–15 of that module.

When two low-noise amplifiers (LNAs) are available for use, as at X-band, the amplifier in the lowest noise configuration is designated as LNA-1. Under some conditions, LNA-2 may be used, and the higher noise temperature values apply.

2.1.3 Pointing Accuracy

Figures 10 and 11 show the effects of pointing error on effective transmit and receive gain of the antenna. These curves are Gaussian approximations based on measured and predicted antenna beamwidths. Data have been normalized to eliminate elevation and wind-loading effects. The equations used to derive the curves are provided in Appendix A.

Table 1. S-Band Transmit Characteristics

Parameter	Value	Remarks
ANTENNA		
Gain at 2070 MHz	55.40 ±0.2 dBi	At elevation angle of peak gain, referenced to feedhorn aperture for matched polarization; no atmosphere included
Transmitter Waveguide Loss	0.6 ±0.1 dB	250 W transmitter output terminal (waterload switch) to feedhorn aperture
Half-Power Beamwidth	0.258 ±0.004 deg	Angular width (2-sided) between half-power points at specified frequency
Polarization	RCP or LCP	Remotely selected.
Ellipticity	1.0 dB (max)	Peak-to-peak axial ratio defined as the ratio of peak-to-trough received voltages with a rotating linearly polarized source and the feed configured as a circularly (elliptically) polarized receiving antenna
Pointing Loss		
Angular	See module 302	Also see Figure 10
CONSCAN	0.03 dB	At S-band, using X-band CONSCAN reference set for 0.1 dB loss
	0.1 dB	At S-band, using S-band CONSCAN reference set for 0.1 dB loss
EXCITER AND TRANSMITTER		
RF Power Output	47.0–54.0, ±0.25 dBm	Referenced to 250-W transmitter output terminal (waterload switch). Settability is limited to 0.25 dB by measurement equipment precision
Power output varies across the bandwidth and may be as much as 0.5 dB below the set value if the frequency is adjusted to a value other than where the power was set. In general, amplitude drift and variation with frequency will be less at higher output power, but specified performance is guaranteed over the operating range of 50 to 250 Watts.		
EIRP (maximum)	108.8, ±0.35 dBm	

Table 1. S-Band Transmit Characteristics (Continued)

Parameter	Value	Remarks
EXCITER AND TRANSMITTER (Continued)		
Frequency Range Covered	2025 to 2110 MHz	
Instantaneous 1-dB Bandwidth	>85 MHz	
Coherent with Earth Orbiter S-Band D/L Allocation	2028.8–2108.7 MHz	240/221 turnaround ratio
Tunability		At transmitter output frequency
Phase Continuous Tuning Range	2.0 MHz	
Maximum Tuning Rate	±12.1 kHz/s	
Frequency Error	0.012 Hz	Average over 100 ms with respect to frequency specified by predicts
Ramp Rate Error	0.001 Hz/s	Average over 4.5 s with respect to rate calculated from frequency predicts
Stability		At transmitter output frequency
Output Power Stability	–0.5, +1.0 dB	From initial calibration value over an 8-h period at a fixed frequency
Group Delay Stability	≤3.0 ns, RMS	Ranging modulation signal path over an 8-h period (see module 203)
Frequency Stability		Allan deviation
1 s	9.0×10^{-13}	
10 s	9.0×10^{-14}	
1000–3600 s	3.0×10^{-15}	
Spurious Output		Below carrier
1–10 Hz	–60 dB	
10 Hz–1.5 MHz	–70 dB	
1.5 MHz–8 MHz	–80 dB	
2nd Harmonic	–80 dB	
3rd, 4th & 5th Harmonics	–90 dB	

Table 2. X-Band Transmit Characteristics

Parameter	Value	Remarks
ANTENNA		
Gain at 7145 MHz	67.05 ±0.2 dBi	At elevation angle of peak gain, referenced to feedhorn aperture for matched polarization; no atmosphere included
Transmitter Waveguide Loss	0.25 ±0.05 dB	20-kW transmitter output terminal (waterload switch) to feedhorn aperture
Half-Power Beamwidth	0.0777 ±0.004 deg	Angular width (2-sided) between half-power points at specified frequency
Polarization	RCP or LCP	One polarization at a time, remotely selected
Ellipticity	1.0 dB (max)	Peak-to-peak axial ratio defined as the ratio of peak-to-trough received voltages with a rotating linearly polarized source and the feed configured as a circularly (elliptically) polarized receiving antenna
Pointing Loss		
Angular	See module 302	Also see Figure 11
CONSCAN	0.1 dB	X-band CONSCAN reference set for 0.1 dB loss
EXCITER AND TRANSMITTER		
RF Power Output	73.0, +0.0, -1.0 dBm	Referenced to 20-kW transmitter output terminal (waterload switch). Settability is limited to 0.25 dB by measurement equipment precision
<p>Power output varies across the bandwidth and may be as much as 1 dB below nominal rating. Performance will also vary from tube to tube. Normal procedure is to run the tubes saturated, but unsaturated operation is also possible. The point at which saturation is achieved depends on drive power and beam voltage. The 20-kW tubes are normally saturated for power levels greater than 63 dBm (2 kW). Minimum power out of the 20-kW tubes is about 53 dBm (200 W). Efficiency of the tubes drops off rapidly below nominal rated output.</p>		
EIRP	139.8, +0.2, -1.0 dBm	

Table 2. X-Band Transmit Characteristics (Continued)

Parameter	Value	Remarks
EXCITER AND TRANSMITTER (Continued)		
Frequency Range Covered	7145 to 7190 MHz	
Instantaneous 1-dB Bandwidth (MHz)	45 MHz	
Coherent with Deep Space S-Band D/L Allocation	7151.9–7177.3 MHz	240/749 turnaround ratio
Coherent with Deep Space S-Band D/L Allocation	7151.9–7188.9 MHz	880/749 turnaround ratio
Tunability		At transmitter output frequency
Phase Continuous Tuning Range	2.0 MHz	
Maximum Tuning Rate	±12.1 kHz/s	
Frequency Error	0.012 Hz	Average over 100 ms with respect to frequency specified by predicts
Ramp Rate Error	0.001 Hz/s	Average over 4.5 s with respect to rate calculated from frequency predicts
Output Power Stability		From initial calibration value over an 8-h period at a fixed frequency
Saturated Drive	± 0.3 dB, peak	
Unsaturated Drive	± 0.5 dB, peak	
Output Power Variation		Across any 2 MHz segment
Saturated Drive	≤ 0.3 dB, p-p	
Unsaturated Drive	≤ 0.5 dB, p-p	
Group Delay Stability	≤ 1.5 ns, RMS	Ranging modulation signal path over 8 h period (see module 203)
Frequency Stability		Allan deviation
1 s	1.0×10^{-12}	
10 s	1.0×10^{-13}	
1000–3600 s	3.0×10^{-13}	

Table 2. X-Band Transmit Characteristics (Continued)

Parameter	Value	Remarks
Spurious Output		Below carrier
1–10 Hz	–50 dB	
10 Hz–1.5 MHz	–60 dB	
1.5 MHz–8 MHz	–45 dB	
2nd Harmonic	–75 dB	
3rd, 4th & 5th Harmonics	–60 dB	

Table 3. S- and X-Band Receive Characteristics

Parameter	Value	Remarks
ANTENNA		
Gain		At elevation angle of peak gain for matched polarization, no atmosphere included. Favorable (+) and adverse (–) tolerances have a triangular PDF. See Figures 2–5 for elevation dependency.
S-Band (2295 MHz)	56.07 ±0.25 dBi	Referenced to feedhorn aperture
X-Band (8420 MHz)	68.41 ±0.2 dBi	Referenced to feedhorn aperture
Half-Power Beamwidth (deg.)		Angular width (2-sided) between half-power points at specified frequency
S-Band	0.242 ±0.020 deg	
X-Band	0.0660 ±0.004 deg	
Polarization		Remotely selected
S-Band	RCP or LCP	
X-Band	RCP or LCP	Same or opposite from transmit polarization
Ellipticity (dB)	0.7 dB	Peak-to-peak voltage axial ratio, RCP and LCP. See definition in Table 1.
S-Band	≤1.0 dB	
X-Band	≤0.8 dB	

Table 3. S- and X-Band Receive Characteristics (Continued)

Parameter	Value	Remarks
ANTENNA (Continued)		
Pointing Loss		
Angular	See module 302	Also see Figures 10 and 11
CONSCAN		
S-Band	0.03 dB, 3 sigma	Loss at S-band when using X-band CONSCAN reference set for 0.1 dB loss at X-band
	0.1 dB, 3 sigma	Recommended value when using S-band CONSCAN reference
X-Band	0.1 dB, 3 sigma	Recommended value when using X-band CONSCAN reference
RECEIVER		
Frequency Ranges Covered (MHz)		
S-Band	2200–2300 MHz	
X-Band		
Telemetry	8400–8500 MHz	
VLBI	8200–8600 MHz	Wideband HEMT LNA
Recommended Maximum Signal Power	-90.0 dBm -70.0 dBm	At LNA input terminal (high-gain mode) AT LNA input terminal (low-gain mode)
Antenna-Microwave Noise Temperature (T_{AMW})		Near zenith, no atmosphere (vacuum) or cosmic noise included. See Table 5 for 25% CD average clear sky noise contribution. Favorable (–) and adverse (+) tolerances have triangular PDF. See Figures 6–9 for elevation dependency.
S-Band (2200–2300 MHz)		With respect to feedhorn aperture
All Stations	34.00 ±2 K	LNA-1, HEMT, non-diplexed path
All Stations	41.76 ±2 K	LNA-1, HEMT, diplexed path

Table 3. S- and X-Band Receive Characteristics (Continued)

Parameter	Value	Remarks
RECEIVER (continued)		
X-Band Dual-HEMT LNAs		With respect to feedhorn aperture
High-Gain Mode		normal configuration
DSS-15, LNA-1, HEMT, RCP	9.68 ±1 K	diplexed, 8200-8600 MHz
DSS-15, LNA-2, HEMT, LCP	10.54 ±1 K	diplexed, 8200-8600 MHz
DSS-15, LNA-1, HEMT, RCP	9.75 ±1 K	diplexed, w/ radar filter, 8200-8500 MHz
DSS-15, LNA-2, HEMT, LCP	10.70 ±1 K	diplexed, w/ radar filter, 8200-8500 MHz
Low-Gain Mode		high spacecraft received power
DSS-15, LNA-1, HEMT, RCP	20.35 ±1 K	diplexed, 8200-8600 MHz
DSS-15, LNA-2, HEMT, LCP	22.18 ±1 K	diplexed, 8200-8600 MHz
DSS-15, LNA-1, HEMT, RCP	30.72 ±1 K	diplexed, w/ radar filter, 8200-8500 MHz
DSS-15, LNA-2, HEMT, LCP	30.79 ±1 K	diplexed, w/ radar filter, 8200-8500 MHz
X-Band Maser/HEMT LNAs, High-Gain Mode, RCP/LCP		
DSS-45	15.47 ±2 K	LNA-1, maser, non-diplexed path, 8400-8500 MHz
DSS-65	15.43 ±2 K	
DSS-45	24.61 ±2 K	LNA-1, maser, diplexed path, 8400-8500 MHz
DSS-65	24.83 ±2 K	
DSS-45	32.37 ±2 K	LNA-2, HEMT, non-diplexed path, 8200-8600 MHz (wide-band)
DSS-65	32.16 ±2 K	
DSS-45	42.00 ±2 K	LNA-2, HEMT, diplexed path, 8400-8500 MHz (narrowed due to diplexer)
DSS-65	41.56 ±2 K	

Table 3. S- and X-Band Receive Characteristics (Continued)

Parameter	Value	Remarks
X-Band Maser/HEMT LNAs, Low-Gain Mode, RCP/LCP		NOTE: Low-gain mode test data not available for DSS-45
DSS-45	$\approx 20.6 \pm 2$ K	LNA-1, maser, non-diplexed path, 8400-8500 MHz
DSS-65	20.52 ± 2 K	
DSS-45	$\approx 29.7 \pm 2$ K	LNA-1, maser, diplexed path, 8400-8500 MHz
DSS-65	29.92 ± 2 K	
DSS-45	$\approx 43.4 \pm 2$ K	LNA-2, HEMT, non-diplexed path, 8200-8600 MHz (wide-band)
DSS-65	43.16 ± 2 K	
DSS-45	$\approx 53.0 \pm 2$ K	LNA-2, HEMT, diplexed path, 8400-8500 MHz (narrowed due to diplexer)
DSS-65	52.56 ± 2 K	
Carrier Tracking Loop Noise B/W	0.25 – 200 Hz	Effective one-sided, noise-equivalent carrier loop bandwidth (B_L)

Table 4. Gain Reduction Due to Wind Loading, 34-m HEF Antennas

Wind Speed		X-Band Gain Reduction (dB)*
(km/hr)	(mph)	
10	6	0.0
30	19	0.01
50	31	0.06
70	43	0.21

* Assumes antenna is maintained on-point using CONSCAN or equivalent closed-loop pointing technique.
S-band gain reduction is less than 0.02 dB for wind speeds up to 70 km/hr.
Worst case, with most adverse wind orientation.

Table 5. T_{AMW} , T_{sky} , and T_{op} for CD=25% Average Clear Weather at Zenith,
Referenced to Feedhorn Aperture

Configuration and Stations	Noise Temperatures, K		
	T_{AMW}	T_{sky}	T_{op}
S-band, all stations, LNA-1, HEMT, non-diplexed	34.00	4.78	38.78
S-band, DSS-45 and DSS-65, LNA-1, HEMT, diplexed	41.76	4.78	46.54
DSS-15 X-band High-Gain Mode (normal configuration):			
X-band, DSS-15, LNA-1, HEMT, RCP, diplexed	9.68	5.04	14.72
X-band, DSS-15, LNA-2, HEMT, LCP, diplexed	10.54	5.04	15.58
X-band, DSS-15, LNA-1, HEMT, RCP, diplexed, w/ narrow-band radar filter	9.75	5.04	14.79
X-band, DSS-15, LNA-2, HEMT, LCP, diplexed, w/ narrow-band radar filter	10.70	5.04	15.74
DSS-15 X-band Low-Gain Mode (high s/c received power):			
X-band, DSS-15, LNA-1, HEMT, RCP, diplexed	20.35	5.04	25.39
X-band, DSS-15, LNA-2, HEMT, LCP, diplexed	22.18	5.04	27.22
X-band, DSS-15, LNA-1, HEMT, RCP, diplexed, w/ narrow-band radar filter	30.72	5.04	35.76
X-band, DSS-15, LNA-2, HEMT, LCP, diplexed, w/ narrow-band radar filter	30.79	5.04	35.83
DSS-45 Maser/HEMT High-Gain Mode, RCP/LCP:			
X-band, DSS-45, LNA-1, maser, non-diplexed	15.47	5.39	20.86
X-band, DSS-45, LNA-1, maser, diplexed	24.61	5.39	30.00
X-band, DSS-45, LNA-2, HEMT, non-diplexed	32.37	5.39	37.76
X-band, DSS-45, LNA-2, HEMT, diplexed	42.00	5.39	47.39
DSS-45 Maser/HEMT Low-Gain Mode, RCP/LCP:			
X-band, DSS-45, LNA-1, maser, non-diplexed	≈ 20.6	5.39	≈ 26.0
X-band, DSS-45, LNA-1, maser, diplexed	≈ 29.7	5.39	≈ 35.1
X-band, DSS-45, LNA-2, HEMT, non-diplexed	≈ 43.4	5.39	≈ 48.8
X-band, DSS-45, LNA-2, HEMT, diplexed	≈ 53.0	5.39	≈ 58.4

Table 5. T_{AMW} , T_{sky} , and T_{op} for CD=25% Average Clear Weather at Zenith,
Referenced to Feedhorn Aperture (Continued)

Configuration and Stations	Noise Temperatures, K		
	T_{AMW}	T_{sky}	T_{op}
DSS-65 Maser/HEMT High-Gain Mode RCP/LCP:			
X-band, DSS-65, LNA-1, maser, non-diplexed	15.43	5.27	20.70
X-band, DSS-65, LNA-1, maser, diplexed	24.83	5.27	29.10
X-band, DSS-65, LNA-2, HEMT, non-diplexed	32.16	5.27	37.43
X-band, DSS-65, LNA-2, HEMT, diplexed	41.56	5.27	46.83
DSS-65 Maser/HEMT Low-Gain Mode, RCP/LCP:			
X-band, DSS-65, LNA-1, maser, non-diplexed	20.52	5.27	25.79
X-band, DSS-65, LNA-1, maser, diplexed	29.92	5.27	35.19
X-band, DSS-65, LNA-2, HEMT, non-diplexed	43.16	5.27	48.43
X-band, DSS-65, LNA-2, HEMT, diplexed	52.56	5.27	57.83

NOTE: X-band low-gain mode test data not available for DSS-45

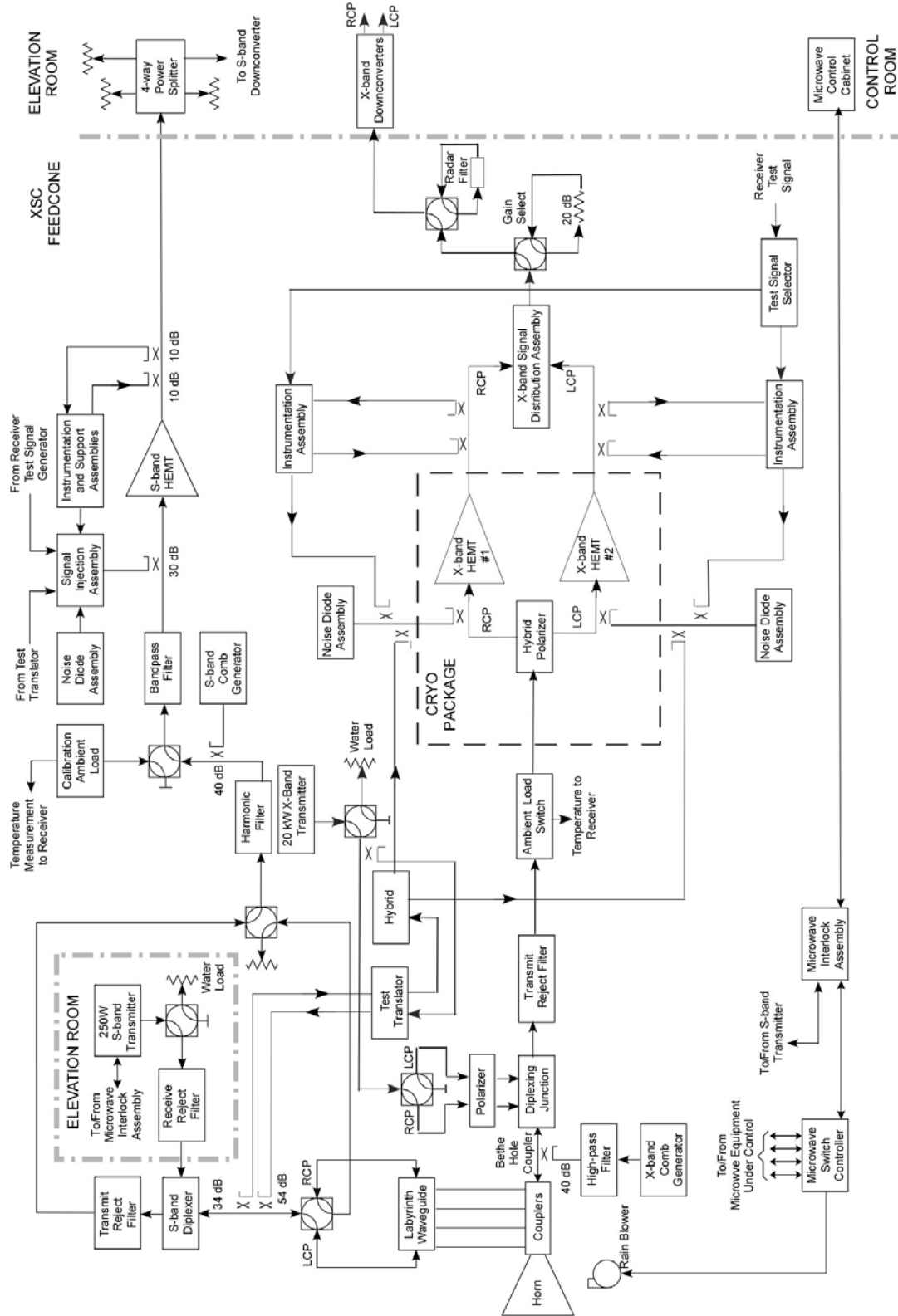


Figure 1a. Functional Block Diagram of the DSS-15 HEF Antenna

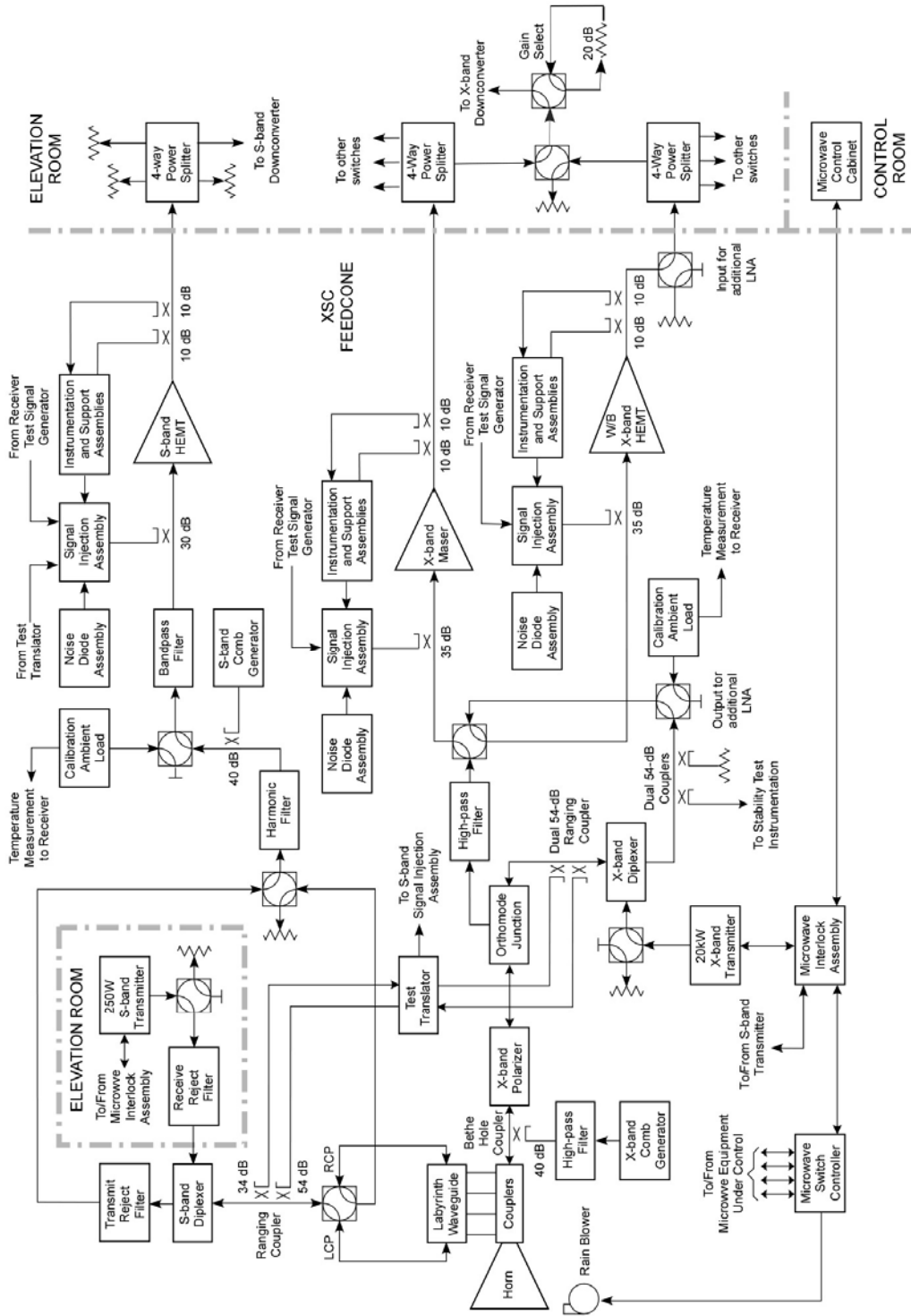


Figure 1b. Functional Block Diagram of the DSS-45 and DSS-65 HEF Antennas

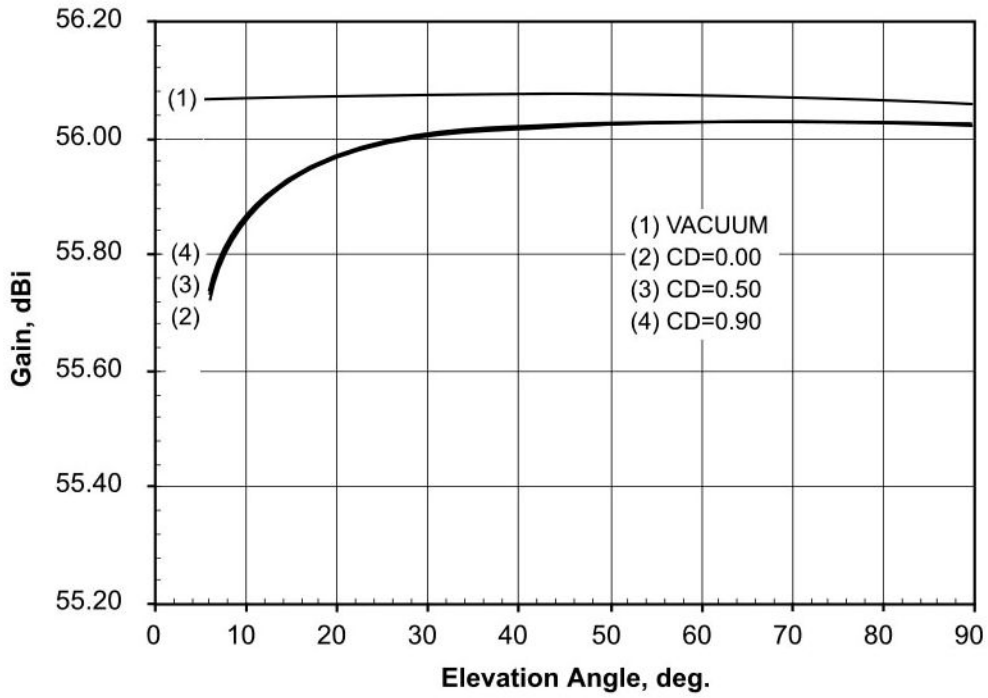


Figure 2. S-Band Receive Gain, All HEF Antennas, at Feedhorn Aperture

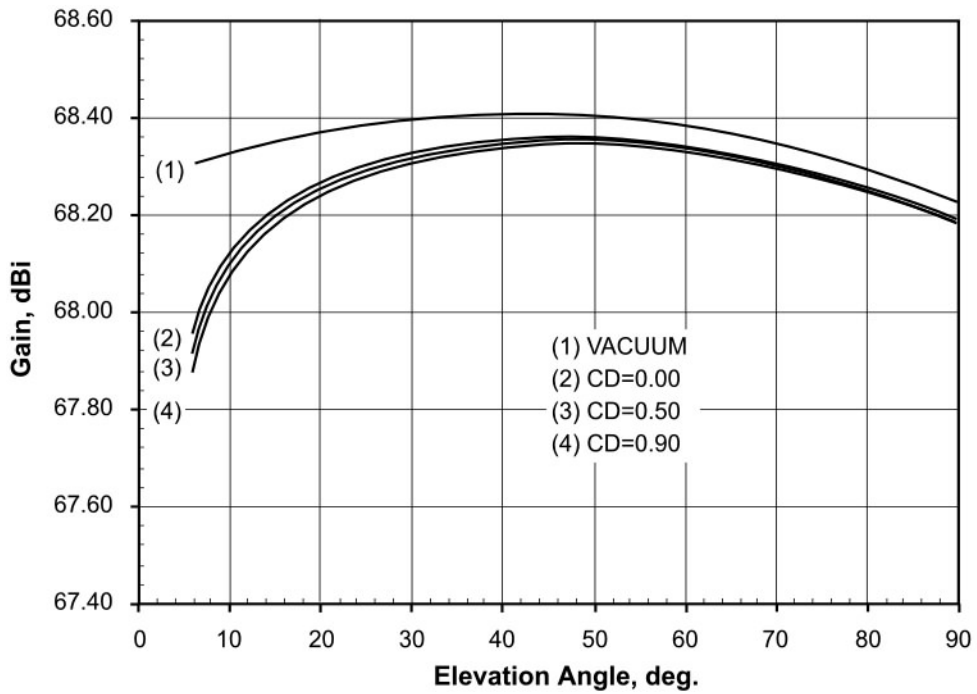


Figure 3. X-Band Receive Gain, DSS-15 Antenna, at Feedhorn Aperture

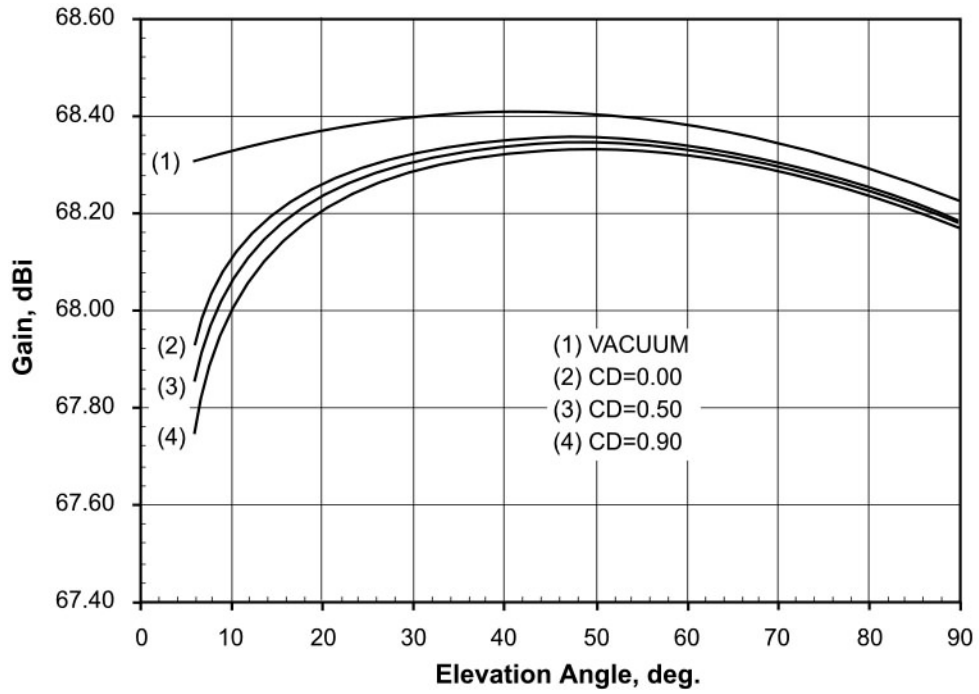


Figure 4. X-Band Receive Gain, DSS-45 Antenna, at Feedhorn Aperture

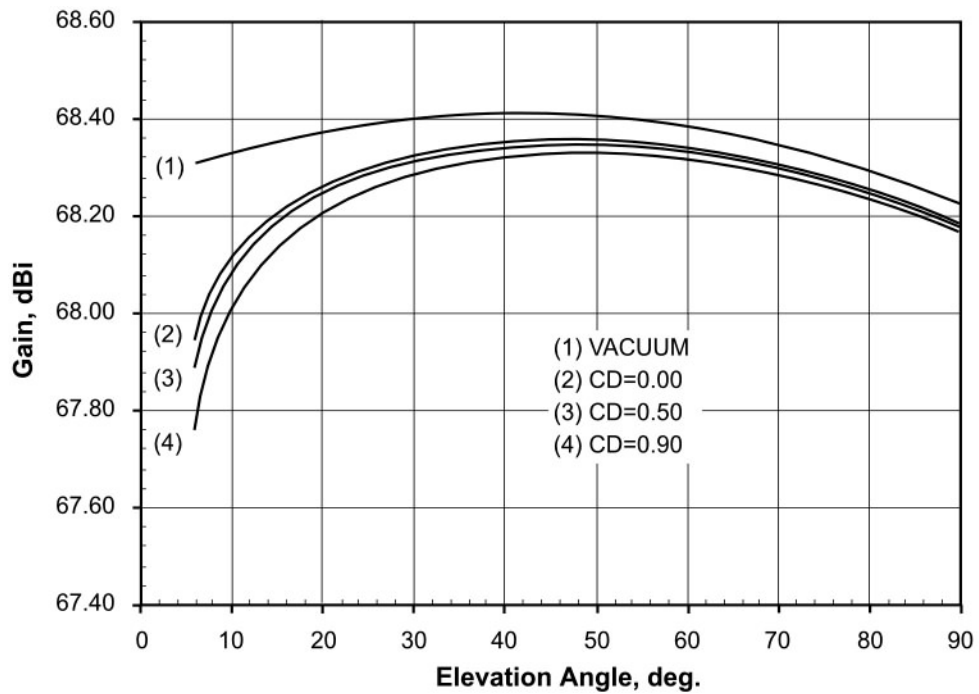


Figure 5. X-Band Receive Gain, DSS-65 Antenna, at Feedhorn Aperture

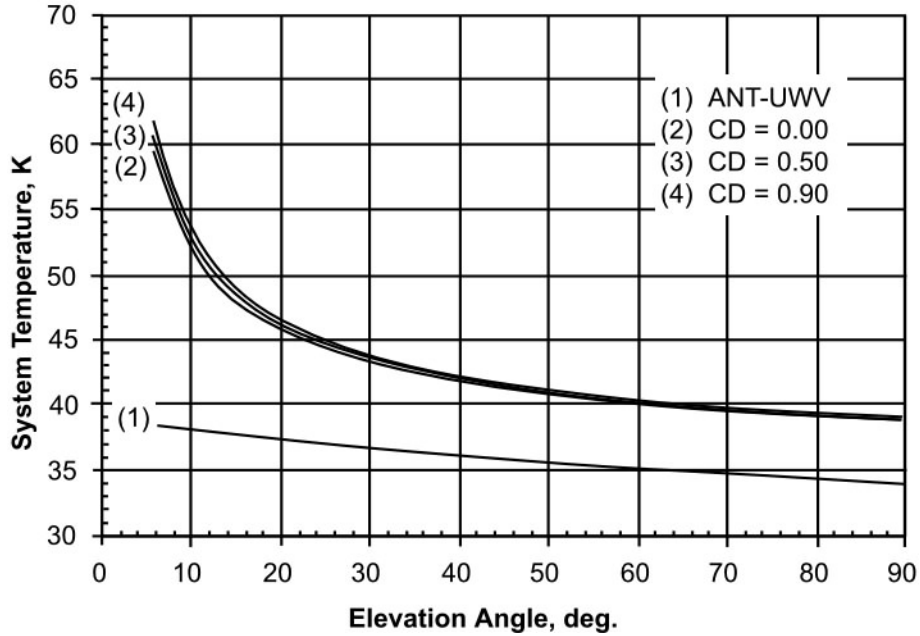


Figure 6. S-band System Noise Temperature, all HEF Antennas, LNA-1, Non-Diplexed, at Feedhorn Aperture

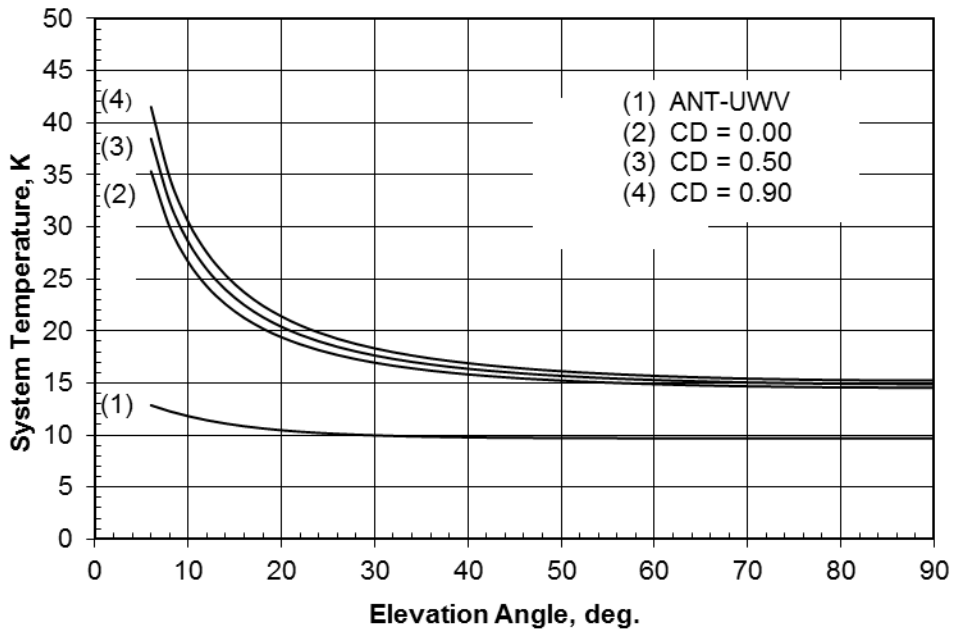


Figure 7. X-Band System Noise Temperature, DSS-15, LNA-1, HEMT, RCP, Diplexed at Feedhorn Aperture

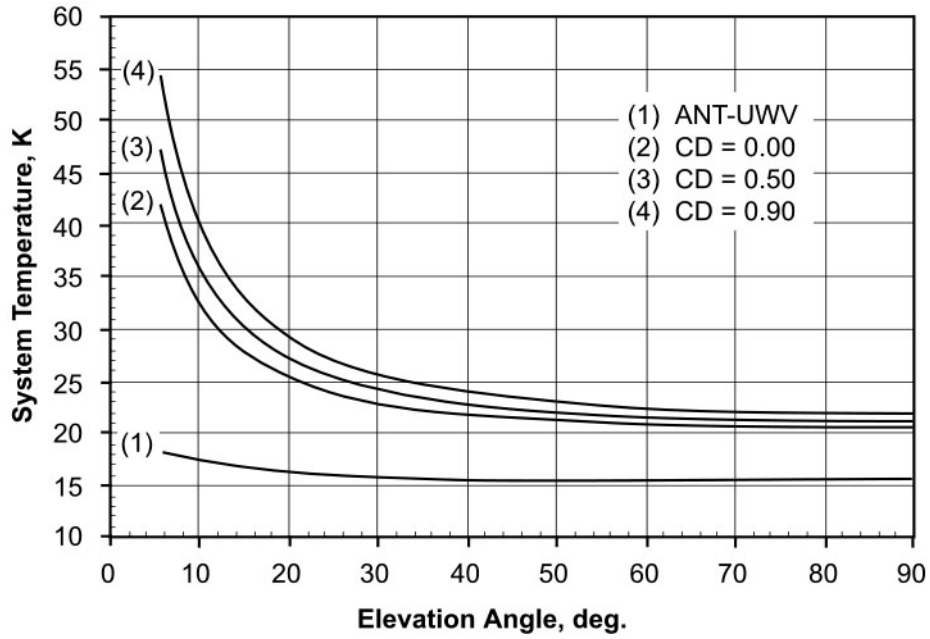


Figure 8. X-Band System Noise Temperature, DSS-45, LNA-1, Non-Diplexed, at Feedhorn Aperture

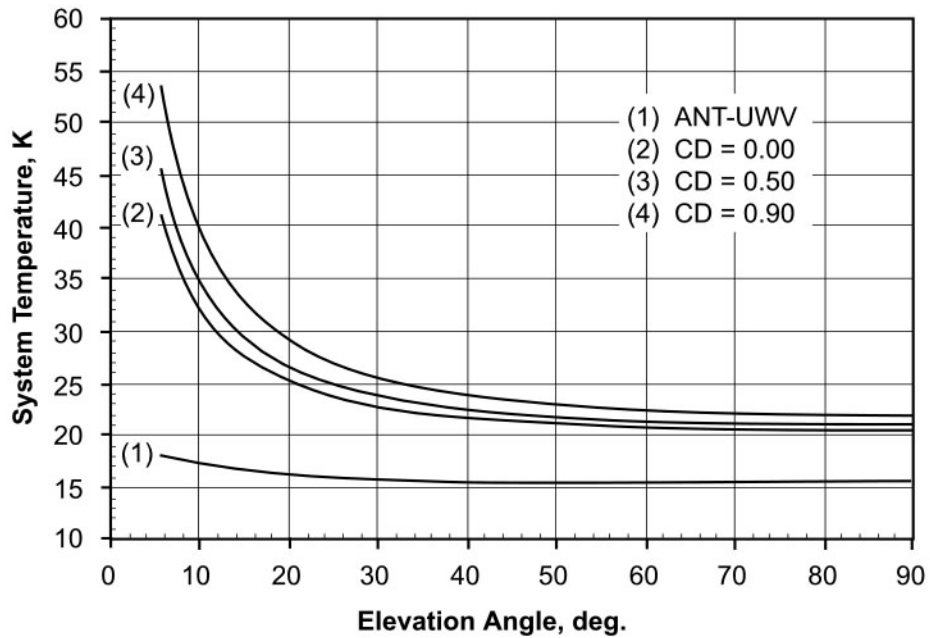


Figure 9. X-Band System Noise Temperature, DSS-65, LNA-1, Non-Diplexed, at Feedhorn Aperture

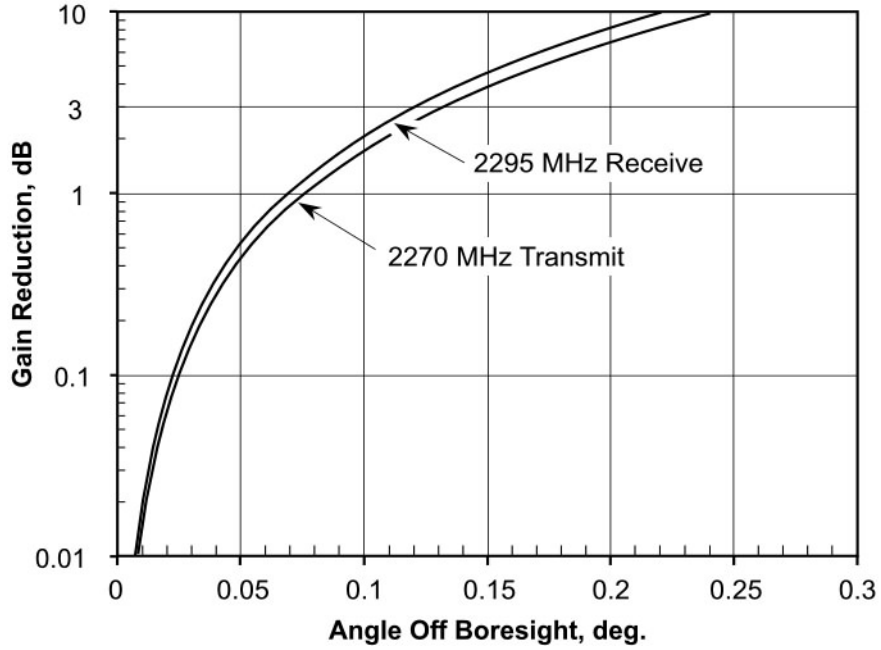


Figure 10. S-Band Gain Reduction Versus Angle Off Boresight

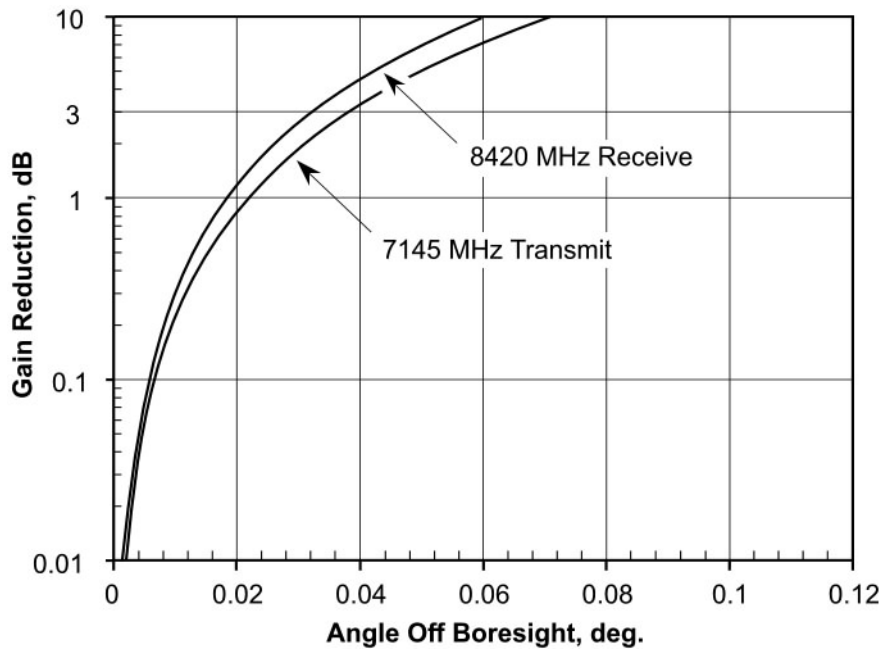


Figure 11. X-Band Gain Reduction Versus Angle Off Boresight

Appendix A ***Equations for Modeling***

A.1 Equations for Gain Versus Elevation Angle

The following equation can be used to generate S- and X-band transmit and receive gain versus elevation curves for DSS-15, DSS-45, and DSS-65. The gains are referenced to the feedhorn aperture, so different configurations (e.g., LNA-1 non-diplexed and LNA-2 diplexed) will have the same gain values. Examples of these curves are shown in Figures 2 through 5, for S- and X-bands. See paragraph 2.1.1.1 for frequency effect modeling and Module 105, Rev. B for atmospheric attenuation at weather conditions corresponding to cumulative distributions from 0% to 99%. The year-average atmosphere attenuations for CD = 0.00, 0.50, and 0.90 are also given in Table A-2.

$$G(\theta) = G_0 - G_1(\theta - \gamma)^2 - \frac{A_{ZEN}}{\sin \theta}, \text{ dBi} \quad (\text{A1})$$

where

θ = antenna elevation angle (deg.) $6 \leq \theta \leq 90$

G_0, G_1, γ = parameters from Table A-1

A_{ZEN} = zenith atmospheric attenuation from Table A-2 or from Tables 10 through 15 in Module 105, dB.

A.2 Equations for System Noise Temperature Versus Elevation Angle

The following equations can be used to generate S-, and X-band receive system noise temperature versus elevation curves for DSS-15, DSS-45, and DSS-65. Examples of these curves are shown in Figures 6 through 9. See Module 105, Rev. B for atmospheric attenuation at weather conditions corresponding to cumulative distributions from 0% to 99%. Atmosphere attenuations for CD = 0.00, 0.50, and 0.90 are also given in Table A-2.

System operating noise temperature:

$$T_{op}(\theta) = T_{AMW} + T_{sky} = \left[T_1 + T_2 e^{-a\theta} \right] + \left[T_{atm}(\theta) + T'_{CMB}(\theta) \right] \quad (\text{A2})$$

Sky noise contribution:

$$T_{sky} = T_{atm}(\theta) + T'_{CMB}(\theta) \quad (\text{A3})$$

Atmospheric attenuation:

$$A(\theta) = \frac{A_{zen}}{\sin(\theta)}, \text{ dB} \quad (\text{A4})$$

Atmospheric loss factor:

$$L(\theta) = 10^{\frac{A(\theta)}{10}}, \text{ dimensionless, } > 1.0 \quad (\text{A5})$$

Atmospheric physical temperature:

$$T_p = 255 + 25 \times CD, \text{ K} \quad (\text{A6})$$

Atmospheric noise contribution:

$$T_{atm}(\theta) = T_p \left[1 - \frac{1}{L(\theta)} \right], \text{ K} \quad (\text{A7})$$

Effective cosmic background noise:

$$T'_{CMB}(\theta) = \frac{T_{CMB}}{L(\theta)}, \text{ K} \quad (\text{A8})$$

where

θ = antenna elevation angle (deg.), $6 \leq \theta \leq 90$

T_1, T_2, a = antenna-microwave noise temperature parameters from Table A-3

A_{ZEN} = zenith atmospheric attenuation, dB, from Table A-2 or from Tables 10 through 15 (S-, X-bands) in Module 105, Rev. B, as a function of frequency, station, and cumulative distribution (CD)

CD = cumulative distribution, $0 \leq CD \leq 0.99$, used to select A_{ZEN} from Table A-2 or from Tables 10 through 15 in Module 105, Rev. B

T_{CMB} = 2.725 K, cosmic microwave background noise temperature

A.3 Equation for Gain Reduction Versus Pointing Error

The following equation can be used to generate gain-reduction versus pointing error curves examples of which are depicted in Figures 10 and 11.

$$\Delta G(\theta) = 10 \log \left(e^{\frac{2.773\theta^2}{HPBW^2}} \right), \text{ dB} \quad (3)$$

where

θ = pointing error (deg.)

$HPBW$ = half-power beamwidth in degrees (from Tables 1, 2, or 3)

Table A-1. Vacuum Component of Gain Parameters

Configuration and Stations	Parameters†			
	G_0^* (Transmit)	G_0^* (Receive)	G_1	γ
S-band, All Stations (Figure 2)	55.40 ‡	56.07	0.000006	42.0
X-band, All Stations (Figures 3—5)	67.05	68.41	0.00008	42.0

NOTES:

† G_0 values are nominal at the frequency specified in Table 1, 2, and 3. Other parameters apply to all frequencies within the same band.

* Favorable tolerance = +0.5 dB, adverse tolerance = -0.5 dB, with a triangular PDF.

‡ S-band uplink G_0 value only applies to DSS 45 and DSS 65 (No S-band uplink at DSS 15).

Table A-2. S- and X-Band Year-Average Zenith Atmosphere Attenuation Above Vacuum (A_{ZEN})

Weather Condition†	A_{ZEN} , dB*					
	S-band			X-band		
	DSS-15	DSS-45	DSS-65	DSS-15	DSS-45	DSS-65
Vacuum	0.000	0.000	0.000	0.000	0.000	0.000
CD = 0.00	0.033	0.036	0.035	0.037	0.039	0.038
CD = 0.50	0.034	0.036	0.035	0.041	0.047	0.044
CD = 0.90	0.034	0.037	0.036	0.045	0.058	0.057

NOTES:

* From Tables 10 through 15 in module 105

† CD = cumulative distribution.

Table A-3. Antenna-Microwave Noise Temperature Parameters, Referenced to Feedhorn Aperture

Configuration and Stations	Parameters		
	T_1^*	T_2	a
S-band , all stations, LNA-1, HEMT, non-diplexed	31.80	7.10	0.013
S-band , all stations, LNA-1, HEMT, diplexed	39.40	7.60	0.013
DSS-15, X-band, High-Gain Mode (normal configuration):			
X-band , DSS-15, LNA-1, HEMT, RCP, diplexed	9.68	5.8	0.1
X-band , DSS-15, LNA-2, HEMT, LCP, diplexed	10.54	5.8	0.1
X-band , DSS-15, LNA-1, HEMT, RCP, diplexed, w/ narrow-band radar filter	9.75	5.8	0.1
X-band , DSS-15, LNA-2, HEMT, LCP, diplexed, w/ narrow-band radar filter	10.70	5.8	0.1
DSS-15, X-band, Low-Gain Mode (high s/c received power):			
X-band , DSS-15, LNA-1, HEMT, RCP, diplexed	20.35	5.8	0.1
X-band , DSS-15, LNA-2, HEMT, LCP, diplexed	22.18	5.8	0.1
X-band , DSS-15, LNA-1, HEMT, RCP, diplexed, w/ narrow-band radar filter	30.72	5.8	0.1
X-band , DSS-15, LNA-2, HEMT, LCP, diplexed, w/ narrow-band radar filter	30.79	5.8	0.1
DSS-45, Maser/HEMT, High-Gain Mode, RCP/LCP:			
X-band , DSS-45, LNA-1, maser, non-diplexed	15.47	5.00	0.10
X-band , DSS-45, LNA-1, maser, diplexed	24.61	6.10	0.10
X-band , DSS-45, LNA-2, HEMT, non-diplexed	32.37	5.50	0.10
X-band , DSS-45, LNA-2, HEMT, diplexed	42.00	6.60	0.10
DSS-45, Maser/HEMT, Low-Gain Mode, RCP/LCP: (**)			
X-band , DSS-45, LNA-1, maser, non-diplexed	≈ 20.6	5.00	0.10
X-band , DSS-45, LNA-1, maser, diplexed	≈ 29.7	6.10	0.10
X-band , DSS-45, LNA-2, HEMT, non-diplexed	≈ 43.4	5.50	0.10
X-band , DSS-45, LNA-2, HEMT, diplexed	≈ 53.0	6.60	0.10

Table A-3. Antenna-Microwave Noise Temperature Parameters, Referenced to Feedhorn Aperture (Continued)

Configuration and Stations	Parameters		
	T_1^*	T_2	a
DSS-65, Maser/HEMT, High-Gain Mode, RCP/LCP:			
X-band , DSS-65, LNA-1, maser, non-diplexed	15.43	5.00	0.10
X-band , DSS-65, LNA-1, maser, diplexed	24.83	6.10	0.10
X-band , DSS-65, LNA-2, HEMT, non-diplexed	32.16	5.50	0.10
X-band , DSS-65, LNA-2, HEMT, diplexed	41.56	6.60	0.10
DSS-65, Maser/HEMT, Low-Gain Mode, RCP/LCP:			
X-band , DSS-65, LNA-1, maser, non-diplexed	20.52	5.00	0.10
X-band , DSS-65, LNA-1, maser, diplexed	29.92	6.10	0.10
X-band , DSS-65, LNA-2, HEMT, non-diplexed	43.16	5.50	0.10
X-band , DSS-65, LNA-2, HEMT, diplexed	52.56	6.60	0.10

NOTES:

* Favorable tolerance = -2 K, adverse tolerance = +2 K, with a triangular PDF.

** Low-gain mode test data not available for DSS-45